ELSEVIER

Cement & Concrete Composites 26 (2004) 787–796

Cement & Concrete Composites

www.elsevier.com/locate/cemconcomp

Experimental and analytical investigation of ferrocement–concrete composite beams

Hani H. Nassif *, Husam Najm

Department of Civil and Environmental Engineering, Rutgers, The State University of New Jersey, 98 Brett Road, Piscataway, NJ 08854, USA

Received 18 November 2002; accepted 22 August 2003

Abstract

The use of cementitious composites for infrastructure applications is becoming more popular with the introduction of new high performance materials. Ferrocement laminates are introduced to enhance the overall performance of structures, such as composite bridge decks, beams, bearing walls, etc. This paper presents the results of an experimental and analytical study done on composite beams made of reinforced concrete overlaid on a thin section of ferrocement (cement paste and wire mesh). In particular, the method of shear transfer between composite layers is examined. Various types of beam specimens with various mesh types (hexagonal and square) are tested under a two-point loading system up to failure. Results from experimental data are compared to those from non-linear analysis as well as a finite element study to model the overall non-linear behavior. Results show that the proposed composite beam has good ductility, cracking strength and ultimate capacity.

Keywords: Ferrocement; Composite; Finite element; Concrete; Deflection; Rehabilitation

1. Introduction

Bridge deck rehabilitation is emerging as an increasingly important topic in the effort to deal with the deteriorating infrastructure. It is by far the major rehabilitation effort in the United States of America (USA). According to a study done by the Federal Highway Administration (FHWA), the number of deficient bridges is increasing mainly due to bridge deterioration and increasingly heavy traffic. It is estimated that 29% of the nation's bridges (more than 542,000) are structurally deficient or functionally obsolete. It will cost an estimated $10.6 billion a year for 20 years to eliminate bridge deficiencies (Federal Highway Administration, FHWA 2000) [1]. Significant bridge deck replacement, rehabilitation and strengthening efforts are underway to decrease the number of deficient bridges. However, the deterioration of bridges grows at a faster rate than repairs are made. The main causes of deterioration of concrete bridge decks are: (1) cracking and spalling of concrete i.e. deck delamination, (2) environmental conditions such as corrosion, and (3) extremely heavy truck loads. Deck delamination and concrete spalling are the most common forms of deterioration. The concrete surface layers become loose and may peel off, exposing the reinforcing steel to the external environment and causing damage to the structure. The use of deicing salts plays a strong role in exacerbating the problem of concrete spalling. Moreover, overweight trucks may lead to deterioration of concrete decks that suffer from delamination or spalling. Nowak et al. [2] gathered data on truck weight (over 600,000-truck record) from Weigh Stations, Weigh-In-Motion measurements, and overweight trucks from the Motor Carrier Division of the Michigan State Police (i.e. citations). Many trucks exceeded the State legal limits on truck gross weight. Heavy load vehicles may shorten the life of the structure. The repeated passage of heavy trucks results in large stress ranges at a large number of cycles. i.e. a shorter fatigue life. Therefore, there is a need to control cracking of bridge decks.

This paper introduces ferrocement laminates with high compressive strength at the bottom of the concrete deck as shown in Fig. 1. The proposed ferrocement layer can be implemented as a repair technique by attaching it to the bottom of an existing structure (e.g. a concrete

* Corresponding author. Tel.: +1-732-445-4414; fax: +1-732-445-8268.

0958-9465/$ - see front matter © 2003 Published by Elsevier Ltd.
doi:10.1016/j.cemconcomp.2003.08.003

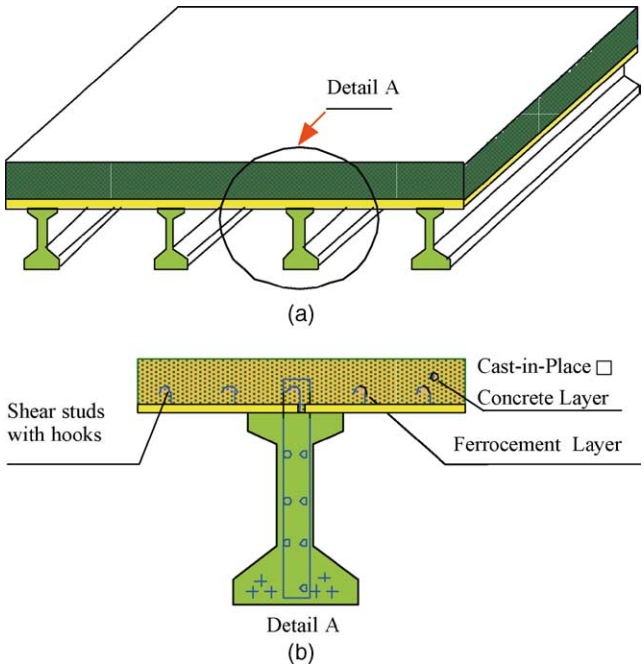

Fig. 1. Proposed application of the ferrocement–concrete composite construction in bridge decks. (a) Composite bridge deck made of R/C and ferrocement. (b) Pre-stressed composite ferrocement-R/C bridge grider.

deck) or as new "stay-in" shoring planks for construction applications. Increasing the compressive strength of the bottom fibers will result in an increase in its tensile strength and modulus of rupture. Consequently, improving the tensile strength of the deck will result in less susceptibility to corrosion, higher cracking capacity, and better fatigue performance. This paper evaluates the performance of such composites under static flexural loading as well as the shear transfer between the ferrocement land reinforced concrete layers. The shear transfer is further examined by considering various types of shear studs and their spacing. Fig. 2 shows four types of shear studs spaced at four different spacing of 914, 457, 305, and 152 mm, respectively. For this purpose, a total of sixteen beams were built and tested. Additionally, a total of eight beams were tested to study the effect of mesh type (hexagonal versus square).

The main constituents of ferrocement are mortar and reinforcement in the form of steel wire mesh. The cementing mix is made of cement and sand mortar while the reinforcement steel wire mesh has openings large enough for adequate bonding. The closer distribution and uniform dispersion of reinforcement, transform the otherwise brittle mortar into a high performance material distinctly different from reinforced concrete. The ACI Committee 549 [3] defined ferrocement as "a type of thin wall reinforced concrete construction where usually hydraulic cement is reinforced with layers of continuous and relatively small diameter mesh". Because the reinforcement is widely distributed throughout the matrix, the material under stress acts approximately as a homogeneous material.

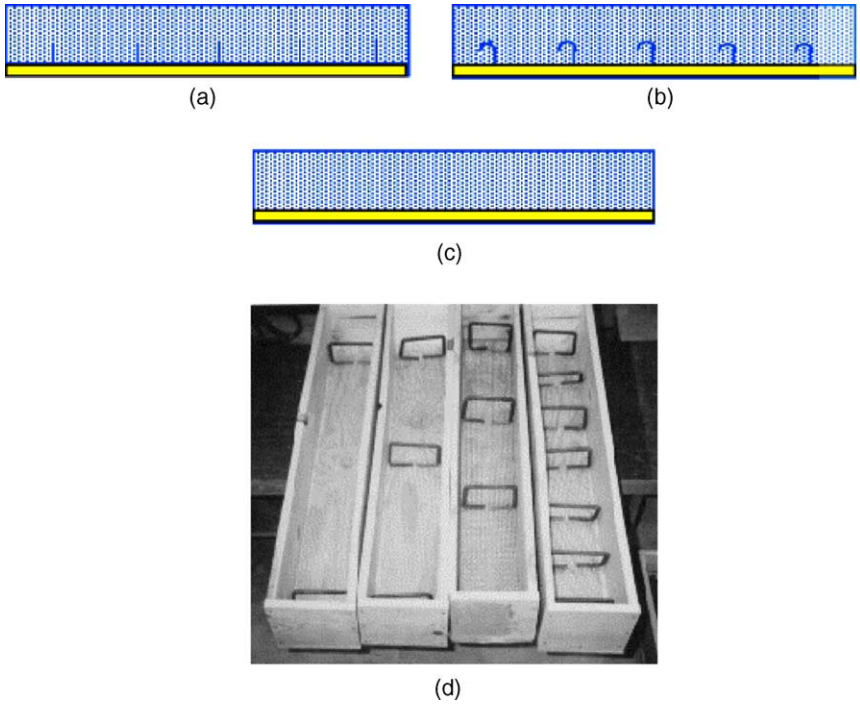

Fig. 2. Various types of shear studs used in this study: (a) "L" type shear stud, (b) "H" type shear studs with hook, (c) rough surface (RS), and (d) "U" type shear studs.

2. Background

Over the last two decades, many researchers initiated studies to determine the mechanical properties of ferrocement as well as its potential use in construction applications. Muhlert [5] showed that the conventional methods used for reinforced concrete analysis are valid to predict load–deflection relationship of ferrocement. Naaman and Shah [4], conducted studies on the tensile properties of ferrocement which indicated that the ultimate load of the composite material was equal to the load carrying capacity of the reinforcement in the loading direction and that the geometry of the mesh influenced the behavior of ferrocement. Naaman and Shah [4] investigated the behavior of ferrocement in uniaxial tension. They considered various parameters such as: fraction volumes of mesh reinforcement, mesh size, mesh diameter, various number of mesh layers, and different types of mesh reinforcement (square woven, welded as well as hexagonal chicken wire mesh). Balaguru [5] studied the experimental behavior of ferrocement in bending. He suggested a mathematical model to predict the moment–curvature and load–deflection relationships of ferrocement beams under flexural loads.

Moreover, to study the composite behavior of ferrocement, Kahn et al. [6] tested forty composite beams made of 0.25 in. thick steel plates and 1 in. thick plates made of either reinforced concrete (R/C) or ferrocement. They concluded the necessity of using sand-blasted plates to improve the composite action between layers. Ramualdi [7] showed that the most important property of ferrocement is its higher cracking resistance capacity which allows for a range of tensile stresses and strains far beyond that of reinforced concrete. Ong and Mansur [8] studied the composite action of steel-deck-reinforced concrete slabs. Eleven one-way slabs were tested. Samples were divided into three groups: group (1) used epoxy resin, group (2) used end anchorage (to ensure composite action) while group (3) used no connectors. Fig. 2 illustrates the shape and arrangement of each group. Samples in all three groups were tested under a two-point loading as well as a uniformly distributed load. It was observed that all samples failed in shear-bond. Specimens in which end anchorages were used as shear transfer devices, showed adequate ductility. It was also shown that it is difficult to achieve full composite action when two different materials are used, such as steel and concrete. This illustrates the need for using two materials that have common or close properties. Mansur and Ong [9] adopted this concept and replaced the steel-deck by ferrocement. The specimens used had no special treatment of the interface between the layers. Seven composite slabs with different reinforcement ratios were tested: three under two-point loading and four under a uniformly distributed load. One of the tested beams failed in bond failure. However, all specimens showed full composite action until failure.

Also, Rosenthal and Bljuger [10] studied the bending behavior of ferrocement as part of a concrete composite materials by testing beams made up of reinforced concrete encased in L-shape high strength ferrocement and reinforced with either rectangular mesh or expanded metal. The interface between the ferrocement and reinforced concrete was relatively smooth. The results showed that loss of bond between the two layers occurred at failure. This implied the need for shear connectors to provide full bond between the two layers at failure.

Tan and Ong [11] studied two different types of composites: (1) beams composed of ferrocement slabs and steel sections, and (2) beams composed of ferrocement slabs and ferrocement sections. Their conclusions pointed to the need for further studies on the behavior of ferrocement sections.

Nassif et al. [12] studied the behavior of ferrocement–concrete composite beams and the required area of steel mesh in the ferrocement layer to ensure overall adequate flexural response in comparison with a similar concrete section. This paper presents the results of beam tests performed to investigate the method of shear transfer between the two composite layers.

3. Finite element analysis

The finite element method in comparison with the most common analytical methods of concrete behavior, is a powerful tool to study the behavior of the proposed ferrocement/reinforced concrete composite beams. A general purpose finite element code, ABAQUS [13], was utilized in this study. ABAQUS includes a variety of routines that allows for the implementation of specific material models (concrete and steel), boundary conditions, and bond behavior. The interaction between the reinforcing steel and concrete is also considered. The concrete material model consists of an isotropically hardening yield surface, active when the stress is dominantly compressive, and an independent "crack detection surface" which determines if a point fails by cracking. The model is a smeared crack model, in the sense that it does not track individual "macro" cracks, but applies the constitutive equations independently at each integration point in the model to determine failure in concrete. The failure criterion is defined by providing the uniaxial tensile and compressive failure stresses as well as the ratio of the biaxial stresses to each uniaxial stress state, respectively. Using these defined stress limits for concrete material, the crack detection surface is developed allowing detection of cracks in each element of the model.

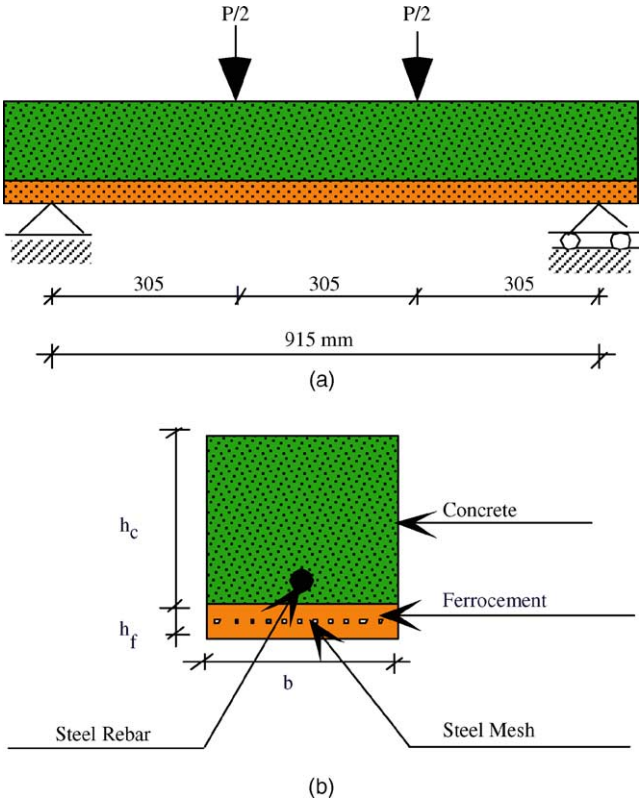

Fig. 3. Typical beam elevation and cross-section considered in this study. (a) Longitudinal view and (b) beam cross-section.

The composite beam used in this study is 914 mm (36 in.) long and subjected to two-point loading as shown in Fig. 3. The beam is composed of two layers: a reinforced concrete (R/C) with a square cross-section dimension of 6 in. and a ferrocement layer with variable thickness. The two layers are assumed to be perfectly bonded along their interface by constraining the same number of nodes in each of the two corresponding layers. Thus, both nodes would have the same degrees of freedom (i.e. displacements and rotations. Practically, full bond can be achieved by introducing adequate number of shear connectors along the interface between both layers. Due to symmetry, only half of the beam was modeled as shown in Fig. 4.

The analysis is performed by applying an incremental load, with iterations in each increment. The modified RIKS algorithm with an assumed proportional loading history is used. This approach determines the static equilibrium solution for unstable response in concrete, due to cracking in tension, yielding of reinforcement, or concrete softening in compression. It neglects any permanent strains associated with cracking. The concrete/steel interface is influenced by effects such as bond slip and dowel action. These effects can be approximated by introducing tension stiffening, which simulates load transfer through the rebar across cracks. The tension stiffening model depends on many factors: the density of

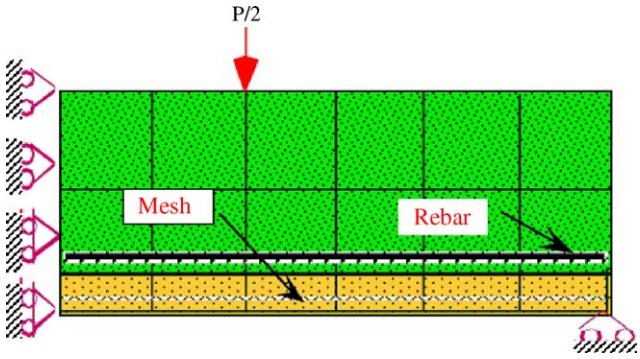

Fig. 4. Finite element model of half composite ferrocement-reinforced concrete beam.

the reinforcement, quality of bond between the concrete and the rebars, the relative size of concrete aggregate compared to the rebar diameter, and mesh size. Also, the reduction in shear stress modulus is introduced as a function of the opening strain across the crack by incorporating shear retention into the model. The tensile strength was taken equal to the modulus of rupture, which is defined by the American Concrete Institute (ACI) as fr, where $fr = 7.5\sqrt{f'c}$.

The analysis was carried out using three different types of elements: beam, shell, and two dimensional plane elements. All three elements yielded the same cracking and ultimate load capacity as shown in Fig. 5. Therefore, a beam element with nine Gaussian integration points is used throughout the parametric study. In order to verify the results obtained from the FEM, a non-linear section analysis was performed. The non-

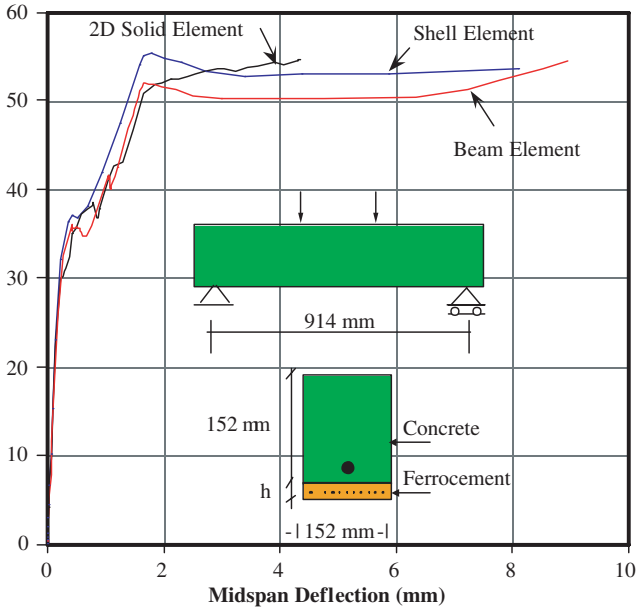

Fig. 5. Load versus deflection for various element types used in the finite element analysis.

linear analysis program is based on the assumption of full bond between both layers. The results are compared in terms of the cracking moment, ultimate moment capacity, and load–deflection as well as moment–curvature relationships.

4. Non-linear analysis

The composite beams are also modeled using a non-linear analysis computer program. The program is used to model both layers assuming full bond. The cracking moment, ultimate moment capacity, moment–curvature relationship, and load–deflection relationship under third point loads can be obtained using this program. The program uses the modified Hognestad model for concrete and typical strain–stress relationships for the reinforcing steel and mesh. The calculation of deflection is based on the curvature of the beam under incremental loading. The beam curvature is determined from the variation of the moment over the span length considering cracking of concrete and yielding of the steel. Results are compared to with those from the finite element model for various percentage of steel mesh reinforcement. Fig. 6 shows a close correlation between both approaches and illustrates that the model can be used to compare with experimental results.

5. Experimental program

The beam specimens were cast in two groups. The dimensions were reduced geometrically from an actual bridge deck. Beams were cast in scaled dimensions of the actual bridge deck slabs between two adjacent girders. The first set of composite beams cast, were of dimensions 152×152×914 mm (6 in.×6 in.×36 in.). The bottom 25.4 mm of these beams was a ferrocement laminate, with steel wire mesh as reinforcement. The top 127 mm of concrete with a No. 10 (No. 3 in US Customary System of units) rebar was cast on top the ferrocement laminate. The rebar was located at 12.7 mm above the ferrocement laminates.

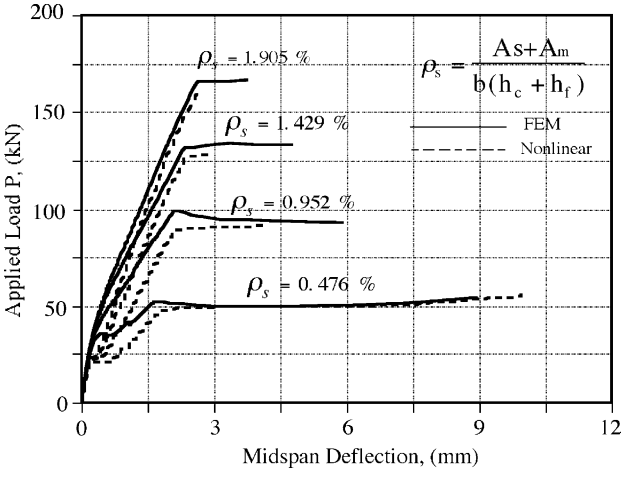

Fig. 6. Comparison of non-linear analysis and finite element method for various percentages of beam reinforcement ratio.

A total of 24 simply supported composite beams were tested under a two-point loading system. All beams are designed to be minimally-reinforced. Details of the beam specimens are summarized in Table 1. The beam specimens are classified into two groups. Group (A1) consists of a total of four beams: three composite beams having 4, 6, and 8 layers of square mesh in the one inch thick ferrocement layer, respectively, and one reinforced concrete beam. Group (A2) consists of a total of four beams: three are composite having 4, 6, and 8 layers of hexagonal mesh in the one inch thick ferrocement layer, respectively, and one reinforced concrete beam. Both groups (B1) and (B2) are reinforced with one (No. 10) rebar as the main reinforcement in the concrete layer. On the other hand, Groups (B10 and (B2) beams have different types of shear studs introduced to study the composite behavior of both layers and the minimum number of studs required to ensure flexural rather bond type of failure.

The mix design used for mortar was according to the guidelines of ACI Committee 549 [3] for design and construction of ferrocement. The mortar was placed in a plywood mold to a depth of one half inch. The molds are placed on a vibrating table to ensure proper compaction and to eliminate any air voids in the mortar. The steel mesh was placed on the mortar with proper spacers to maintain a minimum cover. The top 12.7 mm (half-inch) of the mortar was then placed over the mesh and the mold is vibrated again. Shear studs are provided to prevent horizontal shear failure. The shear studs were made of No. 10 (No. 3) reinforcement and were tied to the mesh prior to casting. For Group A beams, five shear studs were placed at equal distances over the beam span and along the centerline of the ferrocement laminate. The studs were made in the shape of hooks and are 63.5 mm (2.5 in.) long. The final finish of the mortar was kept rough in order to provide bonding with the concrete layer. The ferrocement laminate was cured for 24 h. Cylinders 101.6×203 mm (4 in.×8 in.) were taken to test the compressive strength of the mortar. The volume fraction of the reinforcement for both sets were within the provisions given in the ACI Committee 549 guidelines (Section 4.5), which requires the total volume fraction for non-pre-stressed water retaining structures to be a minimum of 3.5%.

Each No. 3 rebar was installed with one pre-wired strain gage having a gage resistance of 350 ohms. After installation, a protective Teflon tape was used to cover the gage. Finally, a layer of M-Coat J was applied over

Table 1
Properties and details of beam specimen used in tests in groups A and B

Beam no.	Concrete layer						Ferrocement layer					Studs
	b mm	d mm	f'_{cc} MPa	f_{ys} MPa	A_s mm^2	d_s mm	b mm	d mm	f'_{cf} MPa	f_{ym} MPa	No. of layers	No. and spacing mm
A11	152	76	33	413	71	64	152	25.4	38	413	4 Hex.	5 H@ 305
A12	152	76	33	413	71	64	152	25.4	38	413	6 Hex.	5 H@ 305
A13	152	76	33	413	71	64	152	25.4	38	413	8 Hex.	5 H@ 305
A14	152	101	33	413	71	64	–	–	–	–	–	–
A21	152	102	31	413	71	89	152	38	38	413	4 Sq.	5 H@ 305
A22	152	102	31	413	71	89	152	38	38	413	6 Sq.	5 H@ 305
A23	152	102	31	413	71	89	152	38	38	413	8 Sq.	5 H@ 305
A24	152	140	31	413	71	89	–	–	–	–	–	–
B11	152	152	31	413	71	64	152	25.4	38	413	2 Sq.	2 L@ 914
B12	152	152	31	413	71	64	152	25.4	38	413	2 Sq.	3 L@ 457
B13	152	152	31	413	71	64	152	25.4	38	413	2 Sq.	4 L@ 305
B14	152	152	31	413	71	64	152	25.4	38	413	2 Sq.	7 L@ 152
B21	152	152	31	413	71	89	152	25.4	38	413	2 Sq.	2 H@ 914
B22	152	152	31	413	71	89	152	25.4	38	413	2 Sq.	3 H@ 457
B23	152	152	31	413	71	89	152	25.4	38	413	2 Sq.	4 H@ 305
B24	152	152	31	413	71	89	152	25.4	38	413	2 Sq.	7 H@ 152
B25	152	152	31	413	71	89	–	–	–	–	–	Concrete
B31	152	152	31	413	71	89	152	25.4	38	413	2 Sq.	2 RS@ 914
B32	152	152	31	413	71	89	152	25.4	38	413	2 Sq.	2 RS@ 914
B33	152	152	31	413	71	89	152	25.4	38	413	2 Sq.	2 RS@ 914
B34	152	152	31	413	71	89	152	25.4	38	413	–	2 RS@ 914
B41	152	152	31	276	71	89	152	25.4	38	413	2 Sq.	2 U@ 914
B42	152	152	31	413	71	89	152	25.4	38	413	2 Sq.	3 U@ 457
B43	152	152	31	517	71	89	152	25.4	38	413	2 Sq.	4 U@ 305

L = Studs (⌊); H = Studs with hooks (⌒); RS = Rough surface; U = U-shaped studs (⊓).

the gage installation in order to prevent any damage to the strain gage during casting of the beam specimen.

After the ferrocement laminate was cured for three days, the rebar was placed at a cover distance of 12.7 mm (0.5 in.) from the top of the ferrocement layer. The rebar was then placed along the centerline of the beam mold with the strain gage positioned at the bottom of the rebar. Fig. 2(e) shows formwork with typical layout of shear studs pre-attached to the ferrocement mesh. Cylinders were sampled to determine the compressive strength of concrete. The cast beams were removed from the mold after 24 h and placed in a curing tank.

5.1. Testing set-up

The testing of the beams was conducted on a 534 kN (120 kip) Universal Testing Machine (UTM) after 28 days. The clear span of the beams to be tested was 915 mm (36 in.). The two-point loads are applied as shown in Fig. 3a. The beam cross-section is shown in Fig. 3b. Rollers were placed at the required distances to act as supports for the beam. The test bed was equipped with a linear variable differential transducer (LVDT) for recording beam deflection at mid-span. The strain, deflection, and load data were collected using a 16-channel data acquisition system, SOMAT-2100. The SOMAT-2100 system is equipped with a computer module that controls data collected from all channels. The data acquisition system was connected to a desktop computer used to analyze, download, and store the collected data.

5.2. Testing procedure

The testing of all beams was done after 28 days of curing at room temperature under 100% humidity. The cylinders were also cured for 28 days and tested to obtain the compressive strength of concrete and the mortar used for ferrocement. The beams were tested under a two-point loading using a controlled rate of loading. Prior to testing, all channels were calibrated using the automatic calibration procedure available in SOMAT-2100. The testing was conducted until complete failure of the beams. The cracking patterns of the beams were observed.

6. Results

6.1. Composite beam specimens with square mesh layers (group A2 beams)

The load versus mid-span deflection relationship indicates that there are three specific regions: a linear region to yield, a transition region of continuous yield, and a region of full plastic deformation until failure.

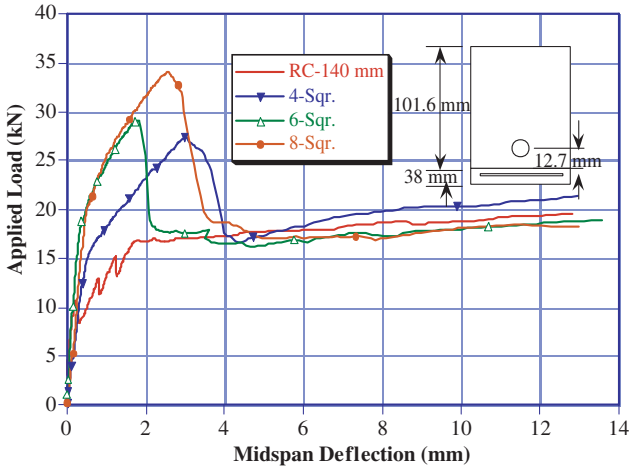

Fig. 7. Applied load versus deflection for group (A2) beams using square mesh.

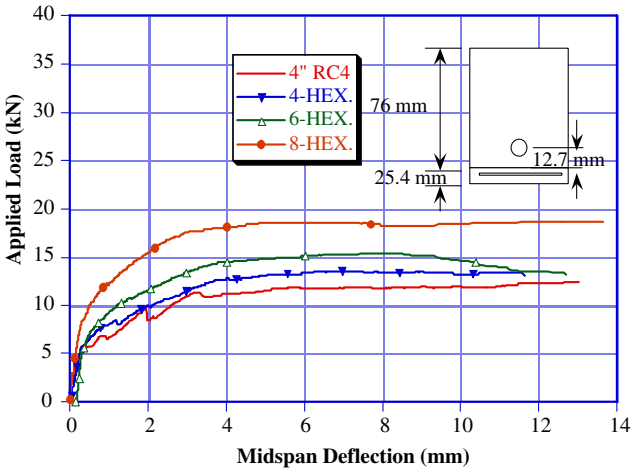

Fig. 8. Applied load versus deflection for group (A1) beams using hexagonal mesh.

Fig. 7 illustrates that the initial stiffness of the composite beams is higher than that of the control R/C beam. The control R/C beam cracked at a load of 9.79 kN (2.2 kips), whereas all composite beams have an initial crack at a load of 17.79 kN (4.0 kip). The cracking behavior indicates that all cracks propagated in the region of maximum moment, i.e., within the two loading points. The peak load for the composite beams ranged between 26.69 and 33.36 kN (6 and 7.5 kips). However, once the composite ferrocement layer develops a major crack, the beam capacity drops to 17.79 kN (4 kip) and behaves similar to the control R/C beam. It was also observed that the steel rebar has already yielded at failure.

6.2. Composite beam specimens with hexagonal mesh layers (group A1 beams)

Fig. 8 shows load versus mid-span deflection relationship for Group (A1) beams. It is observed that the control beam (total height = 101.6 mm (4 in.) has cracked at a lower cracking load (5.34 kN (1.2 kips)) than the composite beams. However, the composite beams did not exhibit a large increase in the cracking stiffness as in the case of group (A2) composite beams. This is attributed to the larger depth of the section. However, there is an increase the stiffness of the composite beams in both groups (A1) and (A2) with the increase in the number of mesh layers.

6.3. Composite beam specimens with L-shaped shear studs (group B1 beams)

Fig. 9 shows the load versus mid-span deflection relationship for beam specimens B11, B12, B14, reinforced concrete beam, finite element method, and non-

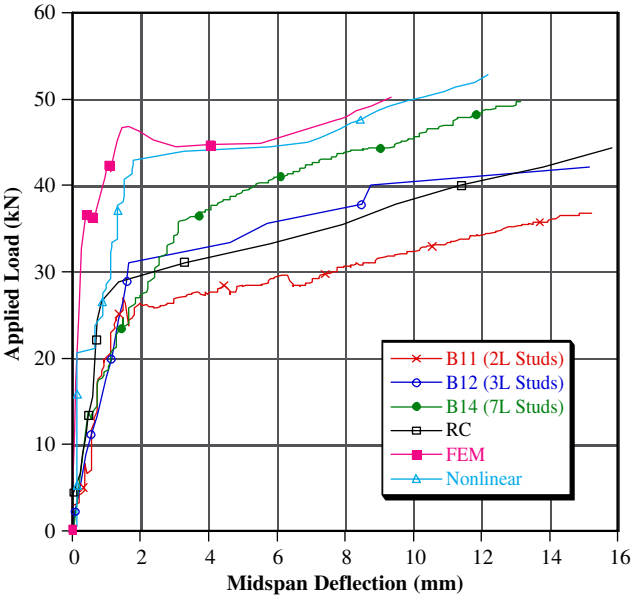

Fig. 9. Applied load versus deflection for group (B1) beams using L-shaped shear studs.

linear analysis. It is observed that up to first cracking, all beams have comparable pre-cracking stiffness. However, each beam has cracked at a different load level. For example, beam B11 starts cracking at 26.69 kN (6.0 kips) at a distance of 406 mm (16.0 in.) from left support. The two layers started de-bonding at a load of 28.46 kN (6.4 kips). Another crack was initiated at a load of 32 kN (7.2 kips) at a distance of 355.6 mm (14 in.) from the right support. Fig. 10 shows beam specimen B11 undergoing bond failure. It is also observed that the first crack in the flexural span of the beam occurs at about 43% of the ultimate load.

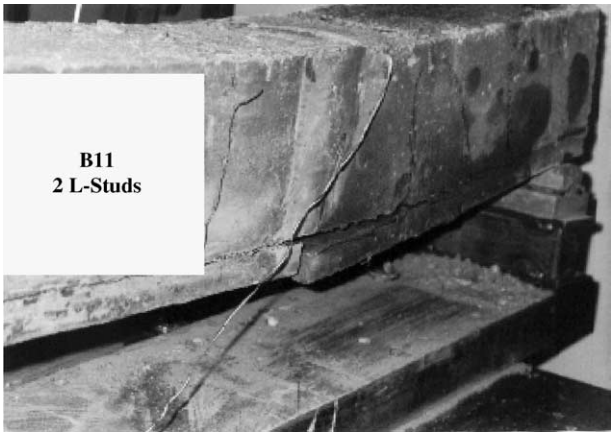

Fig. 10. Bond failure in beam specimen B11 (2L studs) at ultimate.

On the other hand, beam B12 starts cracking at 46.9 MPa at a distance of 38 mm from the left support. The de-bonding between the two layers occurs at a load of 48.2 MPa. For this beam, it is observed that the first crack in the flexural span occurs at about 73% of the ultimate load.

Table 2 shows a comparison of results for group B test at ultimate and cracking limit states. All beams (B11, B12, B13, and B14) have approximately the same ductility and large deflections at the ultimate loading. However, increasing the number of studs resulted in an increase of load carrying capacity of the beams by about 31%. As illustrated in Fig. 9, among all beams, beam B14 (7 L-studs) has achieved a full composite action at ultimate loading (Table 2). Moreover, it is also observed that as a minimum, 4 L-studs are needed to ensure full composite action between the layers. It is also observed that the main steel reinforcement in every beam specimen has reached the yield strength at ultimate as illustrated in Fig. 11.

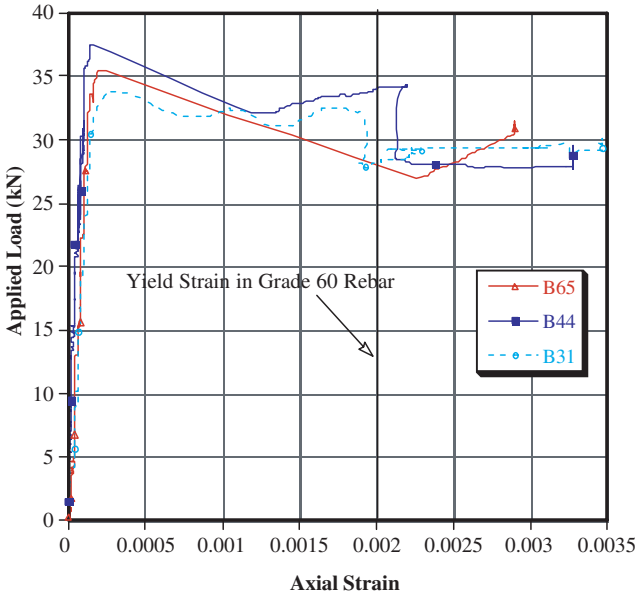

Fig. 11. Applied load versus rebar strain measured using a foil strain gage.

6.4. Composite beam specimens with hooked shear studs (group B2 beams)

Fig. 12 shows the load versus deflection relationship for group B2 beams (B21, B23, and B24), FE model results, non-linear analysis, and concrete control specimen. Similar trend is observed, as was the case in beam group B1. However, the beam B23 (4 Hooks) had a comparable cracking strength as I-Beam B24 (7 hooks) but did not attain its full ultimate strength. Fig. 13 shows that the two layers in B23 have acted with full composite action.

Table 2
Comparison of group B beams—cracking and ultimate loads and maximum deflection

Specimen	Studs spacing (mm)	Cracking load (kN)	Deflection (mm)	Ultimate load (kN)	Deflection (mm)
B11	914 (2 studs)	41.34	1.63	57.19	15.24
B12	457 (3 studs)	46.85	1.52	65.46	14.99
B14	152 (7 studs)	42.03	2.00	72.35	13.97
B21	914 (2 Studs with hook)	50.30	1.00	64.77	16.26
B23	305 (4 Studs with hook)	48.23	0.51	65.46	15.75
B24	152 (7 Studs with hook)	50.30	0.53	81.30	14.48
B31	914 (Rough)	41.34	2.90	50.30	14.99
B32	914 (Rough)	41.34	2.87	55.12	16.26
B34	914 (Rough)	41.34	3.56	53.88	15.49
B41	914 (2 U studs)	48.23	1.00	48.71	9.65
B42	305 (4 U studs)	47.54	1.19	54.43	11.94
B43	152 (7 U studs)	43.41	2.18	55.12	15.00
B51	914 (2 Shear keys)	37.21	1.37	47.20	14.48
B53	305 (4 Shear keys)	37.21	0.48	72.35	7.37
B61	914 (Glue)	42.72	1.02	57.53	8.38
B62	914 (Glue)	41.34	0.82	55.12	8.64
B64	914 (Glue)	40.65	2.84	57.53	7.87

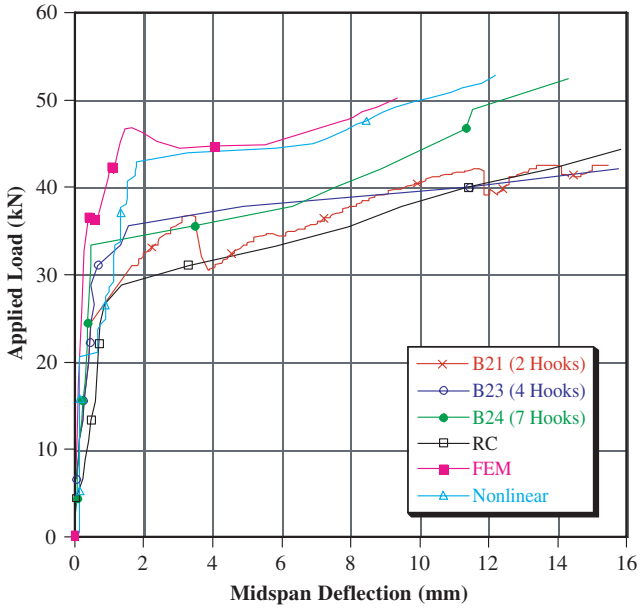

Fig. 12. Applied load versus deflection for group (B2) beams using shear studs with hooks.

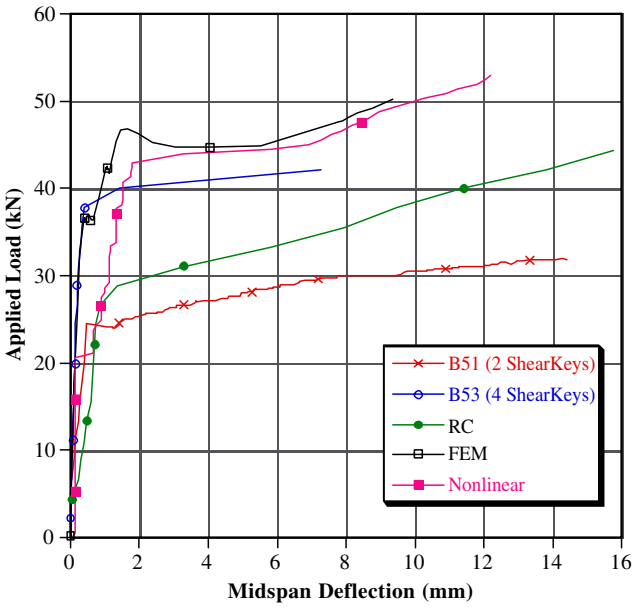

Fig. 14. Applied load versus deflection for group (B5) beams using shear keys.

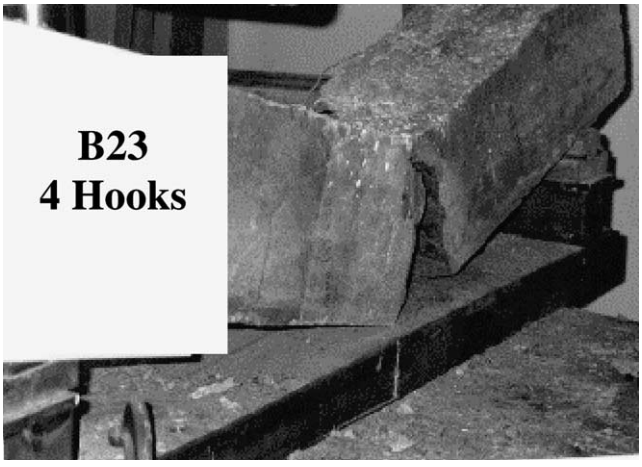

Fig. 13. Beam B23 (4 hooks) after complete failure.

6.5. Composite beam specimens with shear keys (group B5 beams)

Fig. 14 shows that for group B5 (Shear keys) a minimum of 4 shear keys was needed to ensure full composite action between both composite layers. However, it observed that after the beam reached its cracking capacity, there was a loss in ductility in comparison with the control specimen. For brevity only these beam groups are presented, however, similar trends have been observed.

7. Conclusions and recommendations

Based on the above results, the following conclusions are made:

1. Full composite action between both layers can not be attained based on rough surfaces without shear studs. It was observed that a minimum number of five studs is needed to provide full composite action between both layers.
2. Beams having shear studs with hooks (Group B2) exhibited better pre-cracking stiffness as well as cracking strength than those with L-shaped studs (Group B1).
3. Beam specimens with square mesh (Group A1) exhibited better cracking capacity than the control beam as well as beams with hexagonal mesh (Group A2). However, the change in the ultimate capacity was not significant.
4. The FEM predicted the ultimate moment capacity for composite beams given that adequate number of shear connectors is provided to ensure full bond until failure. However, the model needs to address partial bond between layers resulting from inadequate shear transfer.
5. Using the procedure adopted in casting these composite beams, it is feasible to produce this type of pre-cast elements for field applications.

Acknowledgements

The authors would like to acknowledge the help of their former graduate students Mark Sanders, Mostafa Mostafa, and Nasser Abdul-Rahman for their help in this study.

References

[1] FHWA, The State of The Nation's Highway and Bridges: Condition and Performance and Highway Bridge Replacement and Rehabilitation Program, Federal highway Administration, US Department of Transpiration, Washington, DC, 1998.
[2] Nowak AS, Nassif HH, DeFrain L. Effect of truck loading on girder bridges. J Transport Eng, ASCE 1993;119(6):853–67.
[3] ACI Committee 549 report, State of the Art Report on Ferrocement, ACI 549-93, 1993.
[4] Naaman AE, Shah SP. Tensile tests of ferrocement. ACI Struct J 1971:693–8.
[5] Balaguru PN. Ferrocement in bending. PhD Thesis, University of Illinois at Chicago Circle, the Graduate College, 1977. p. 9–24.
[6] Kahn LF, Townsend WH, Kaldjian MJ. Ferrocement steel-plate composite beams. ACI J 1975;72(3):94–7.
[7] Romualdi JP. Research needs and the future of ferrocement. Article in "Ferrocement-Material and Application", Publication, SP-61, ACI, Detroit, 1979. p. 173–7.
[8] Ong KCG, Mansur MA. A Study of steel-deck-reinforced concrete slabs. In: Preceding of the Ninth Australian Conference on the Mechanics of Structures and Materials, The University of Sydney, 1984.
[9] Mansur MA, Ong KCG. Composite behavior of ferrocement-deck-reinforced concrete slabs. J Ferrocement 1986;16(1):13–22.
[10] Rosenthal I, Bljuger F. Bending behavior of ferrocement-reinforced concrete composite. J Ferrocement 1985;15(1):15–24.
[11] Tan KH, Ong KCG. Use of ferrocement in composite construction. In: International Conference on Steel and Aluminum Structures, 22–24 May 1991.
[12] Nassif HH, Chirravuri G, Sanders M. Flexural behavior of ferrocement/concrete composite beams. In: Naaman AE, editor. Ferrocement 6: Lambot Symposium, Proceedings of Sixth International Symposium on Ferrocement. University of Michigan, Ann Arbor, June, 1998. p. 251–8.
[13] ABAQUS Manuals. User's Manuals, Version 5.8. Hibbitt, Karlsson, and Sorensen, Inc., 2000.